

Article

Technoeconomic Analysis for Green Hydrogen in Terms of Production, Compression, Transportation and Storage Considering the Australian Perspective

M. Shahabuddin ^{1,2,*} , M. A. Rhamdhani ^{1,2}  and G. A. Brooks ^{1,2} 

¹ Victorian Hydrogen Hub (VH2), Swinburne University of Technology, Hawthorn, VIC 3122, Australia; arhamdhani@swin.edu.au (M.A.R.); gbrooks@swin.edu.au (G.A.B.)

² FPD (Fluid and Process Dynamics) Group, Department of Mechanical and Product Design Engineering, Swinburne University of Technology, Hawthorn, VIC 3122, Australia

* Correspondence: sahammad@swin.edu.au

Abstract: This current article discusses the technoeconomics (TE) of hydrogen generation, transportation, compression and storage in the Australian context. The TE analysis is important and a prerequisite for investment decisions. This study selected the Australian context due to its huge potential in green hydrogen, but the modelling is applicable to other parts of the world, adjusting the price of electricity and other utilities. The hydrogen generation using the most mature alkaline electrolysis (AEL) technique was selected in the current study. The results show that increasing temperature from 50 to 90 °C and decreasing pressure from 13 to 5 bar help improve electrolyser performance, though pressure has a minor effect. The selected range for performance parameters was based on the fundamental behaviour of water electrolysers supported with literature. The levelised cost of hydrogen (LCH₂) was calculated for generation, compression, transportation and storage. However, the majority of the LCH₂ was for generation, which was calculated based on CAPEX, OPEX, capital recovery factor, hydrogen production rate and capacity factor. The LCH₂ in 2023 was calculated to be 9.6 USD/kgH₂ using a base-case solar electricity price of 65–38 USD/MWh. This LCH₂ is expected to decrease to 6.5 and 3.4 USD/kgH₂ by 2030 and 2040, respectively. The current LCH₂ using wind energy was calculated to be 1.9 USD/kgH₂ lower than that of solar-based electricity. The LCH₂ using standalone wind electricity was calculated to be USD 5.3 and USD 2.9 in 2030 and 2040, respectively. The LCH₂ predicted using a solar and wind mix (SWM) was estimated to be USD 3.2 compared to USD 9.6 and USD 7.7 using standalone solar and wind. The LCH₂ under the best case was predicted to be USD 3.9 and USD 2.1 compared to USD 6.5 and USD 3.4 under base-case solar PV in 2030 and 2040, respectively. The best case SWM offers 33% lower LCH₂ in 2023, which leads to 37%, 39% and 42% lower LCH₂ in 2030, 2040 and 2050, respectively. The current results are overpredicted, especially compared with CSIRO, Australia, due to the higher assumption of the renewable electricity price. Currently, over two-thirds of the cost for the LCH₂ is due to the price of electricity (i.e., wind and solar). Modelling suggests an overall reduction in the capital cost of AEL plants by about 50% in the 2030s. Due to the lower capacity factor (effective energy generation over maximum output) of renewable energy, especially for solar plants, a combined wind- and solar-based electrolysis plant was recommended, which can increase the capacity factor by at least 33%. Results also suggest that besides generation, at least an additional 1.5 USD/kgH₂ for compression, transportation and storage is required.

Keywords: hydrogen generation; hydrogen transportation; hydrogen compression; hydrogen storage; technoeconomics



Citation: Shahabuddin, M.; Rhamdhani, M.A.; Brooks, G.A. Technoeconomic Analysis for Green Hydrogen in Terms of Production, Compression, Transportation and Storage Considering the Australian Perspective. *Processes* **2023**, *11*, 2196. <https://doi.org/10.3390/pr11072196>

Academic Editor: Paola Ammendola

Received: 30 May 2023

Revised: 17 July 2023

Accepted: 18 July 2023

Published: 21 July 2023



Copyright: © 2023 by the authors. Licensee MDPI, Basel, Switzerland. This article is an open access article distributed under the terms and conditions of the Creative Commons Attribution (CC BY) license (<https://creativecommons.org/licenses/by/4.0/>).

1. Introduction

Hydrogen is vital in various industrial applications, including enhancing and purifying crude oil and as a precursor for chemicals such as methanol, ammonia and dimethyl

ether. Hydrogen has recently been used as carbon-free fuels and reductants in mobility and green steel manufacturing. Currently, 90 million tonnes (Mt) of hydrogen is produced [1], out of which 59.7% is produced using steam methane reforming, 19% is from coal gasification, 0.6% is from oil reforming and the remaining 20.7% is from the crude by-product of naphtha reforming [1]. A minor amount of hydrogen is produced from renewable electrolysis technology. The worldwide consumption of hydrogen is rising at a rate of approximately 3–4% every year, primarily due to the increased demand for transportation fuels [2] and greater use in steel industries [3]. The major demand for hydrogen includes ammonia production (65%), methanol production (25%), direct reduced iron production (10%) and less than 1% for other purposes [1].

According to the IEA net zero emission target, hydrogen demand is forecasted to increase 6-fold to 530 Mt by 2050 [1]. However, hydrogen production contributes to a large amount of CO₂ emission (900 MtCO₂ per year), i.e., about 2.5% of the global emission from the energy and industry sector due to the current dominant hydro-carbon-based hydrogen production [1]. For example, steam methane reforming emits about 9–11 kgCO₂ per kg of hydrogen [4,5]. Hence, a recent push worldwide is to produce green hydrogen from water electrolysis using green electricity such as solar and PV, especially from excess renewable electricity [6]. However, the widespread adoption of renewable energy sources (RESs) has the potential to negatively impact grid stability due to their fluctuating and uncertain nature [7]. To address this issue, hydrogen has been proposed as a significant energy storage solution on a large scale, utilising the process of water electrolysis [8].

There are four main technologies used for the electrolysis of water, including alkaline electrolysis, anion exchange membrane (AEM) electrolysis, proton exchange membrane (PEM) electrolysis and solid oxide electrolysis (SOE) [9]. Of those, alkaline electrolysis is the most mature and available for large-scale hydrogen production [10]. The cost of the alkaline electrolyser varies over 1000–5000 USD/kW with a production capacity of 1 to 760 Nm³/h [11]. An ordinary alkaline electrolysis cell comprises two Ni-based electrodes placed in a liquid electrolyte, typically a water solution of 30–35 wt.% KOH and separated by a porous diaphragm. The cell operates between 60 and 90 °C, and the pressure is usually below 30 bar. The hydrogen produced by this process has a purity level between 99.5% and 99.9%, which can be further enhanced up to 99.999% by catalytic gas purification systems [12].

Despite the availability and lower specific cost, alkaline electrolysis suffers from low current density (A/cm²) and lower efficiency and durability [8,10,12,13] as a result of electrode overvoltage [14,15], higher ohmic loss [16] and corrosive electrolyte [16,17]. The objective of this study is two-fold. In the first part of the study, we developed mathematical modelling to understand the fundamental physics of the electrolysis system. Secondly, we conducted a techno-economic study of the alkaline electrolysis-based hydrogen generation, transportation, compression and storage system.

Salkuyeh et al., 2018 [4] studied the techno-economics of hydrogen production from different biomass gasification. Their results showed that the cost of hydrogen ranges over 3–3.5 USD/kgH₂ using a biomass-based system and is about 1.0 USD/kgH₂ using steam methane reforming (SMR) without carbon capture and storage (CCS). Zghaibeh et al., 2022 [18] conducted techno-economic modelling for a PV solar-based hydrogen generation system. The results showed that the levelised cost of hydrogen (LCH₂) using a 5 MWp plant is 6.2 EUR/kg with a break-even period of 8 years. Benalcazar and Komorowska, 2022 [19] performed a techno-economic analysis for a PEM hydrogen energy system and showed that the LCH₂ in Poland ranges from 6.37 to 13.48 EUR/kg in 2020 and might decrease to 2.33 to 4.30 EUR/kg in 2030 and 1.23 to 2.03 EUR/kg in 2050. Considering the Italian scenario, Minutillo et al., 2021 [20] studied the LCH₂ in refuelling stations with onsite hydrogen production via water electrolysis. The LCH₂ was reported to be EUR 9.29 to EUR 12.48 per kg. Another study by Fragiaco and Genovese [21] reported that the LCH₂ ranges from EUR 6.90 to EUR 9.85 per kg, considering the Italian context. Lee et al., 2023 [22] reported an optimum LCH₂ of 12.86 USD/kgH₂ using a concentrated

solar-powered hydrogen production system. Babarit et al., 2018 [23] studied the techno-economic modelling of offshore wind-based hydrogen production systems, including transportation and distribution. In the shorter term, the cost of hydrogen was reported to be 7.1–9.4 EUR/kgH₂ using the electricity price of 0.08 EUR/kWh, which in the long run would be 3.5 to 5.7 EUR/kg with the cost of electricity of 0.04 EUR/kWh. Ibagon et al., 2023 [24] reported a much lower LCH₂ ranging from 3.5 USD/kgH₂ in 2022 to 2.3 USD/kgH₂ in 2030.

Recently, Jang et al., 2022 [25] studied the LCH₂ for four different water electrolysis systems, including alkaline water electrolysis (AWE), proton exchange membrane electrolysis (PEMEC), solid oxide electrolysis with electric heaters (SOEC-EH) and solid oxide electrolysis combined with a waste heat source (SOEC-WH). The results showed that the LCH₂ values for AWE, PEMEC, SOEC-EH and SOEC-WH are 7.60, 8.55, 10.16 and 7.16 USD/kgH₂, respectively. The levelised cost of hydrogen generation, transportation and storage depends on various factors, including electricity price, travel distance, transportation mode and technology choice [24]. Table 1 summarises the techno-economic modelling available in the literature.

Table 1. Summary of the techno-economic modelling in the literature (euro to dollar: 1.12).

References	Methods	Key Findings
Salkuyeh et al., 2018 [4]	Biomass gasification-based H ₂ production	LCH ₂ : 3–3.5 USD/kgH ₂
Zghaibeh et al., 2022 [18]	PV solar-based H ₂ production	LCH ₂ : ~7 USD/kgH ₂
Benalcazar et al., 2022 [19]	PEM water electrolysis H ₂ production	LCH ₂ : ~7–15 USD/kgH ₂
Minutillo et al., 2021 [20]	Water electrolysis-based H ₂ production	LCH ₂ : ~10–14 USD/kgH ₂
Fragiacomo and Genovese, 2020 [21]	PEM water electrolysis H ₂ production	LCH ₂ : ~7.75–11 USD/kgH ₂
Lee et al., 2023 [22]	CSP-based solar H ₂ production	LCH ₂ : ~14.4 USD/kgH ₂
Babarit et al., 2018 [23]	Offshore wind-based H ₂ production	LCH ₂ : ~8–10.5 USD/kgH ₂
Ibagon et al., 2023 [24]	Off-grid green H ₂ production	LCH ₂ : ~3.5 USD/kgH ₂
Jang et al., 2022 [25]	Different electrolysis-based H ₂ production	LCH ₂ : ~7.0–10 USD/kgH ₂

Numerous studies in the literature discussed the technoeconomics of green hydrogen, particularly considering the European context [19,20]. However, limited studies are available in the open literature for detailed technoeconomics of green hydrogen for the Australian context. Furthermore, the levelised cost of hydrogen for transportation, compression and storage is rare in the literature besides generation. Moreover, Sanchez et al., 2020 [10] recently studied the alkaline electrolysis (AEL) system for hydrogen production using Aspen Plus and mathematical modelling with experimental validation. The results revealed that increasing stack temperature but decreasing pressure helped improve the stack performance and suggested that techno-economic modelling is necessary to elucidate the system viability fully.

Although the fundamental study of AEL and techno-economic modelling are not directly co-related, some overview of AEL performance parameters may help the reader understand factors affecting its performance. Hence, in this study, in addition to briefly discussing the fundamental aspect of AEL electrolysis-based hydrogen production, we endeavour to highlight techno-economic analysis for hydrogen generation, compression, transportation and storage, especially considering the Australian context.

2. Methodology

2.1. Fundamental Equations in Producing Hydrogen Using Alkaline Electrolysis

Equations listed in Table 2 were employed to carry out the mathematical modelling. A detailed explanation of those equations can be found in Sanchez et al., 2020 [10]. Hence, this section only explains the key parameters briefly.

Table 2. Key equations used for the modelling of AEL.

Decomposition of water	$\text{H}_2\text{O} \rightarrow \text{H}_2 + \frac{1}{2}\text{O}_2$	(1)
Cell voltage	$V(\text{Cell}) = V(\text{rev}) + (r1 + r2 \times T)i + s \times \log \left[\left(t1 + \frac{t2}{T} + \frac{t3}{T^2} \right) \times i + 1 \right]$	(2)
Faradic efficiency	$\eta_F = \frac{\eta_{\text{H}_2 \text{ Produced}}}{\eta_{\text{H}_2 \text{ theoretical}}}$	(3)
Faraday's efficiency	$\eta_F = \left(\frac{i^2}{f_{11} + f_{12} \times T + i^2} \right) \times (f_{11} + f_{22} + T)$	(4)
Hydrogen to oxygen	$\begin{aligned} (\text{HTO}) = \\ (C1 + C2 \times T + C3 \times T^2(C4 + C5 \times T + C6 \times T^2) \times \text{EXP}(C7 + C8 \times T + C9 \times T^2)/i) + \\ (E1 + E2 \times p + E3 \times p^2(E4 + E5 \times p + E6 \times p^2) \times \text{EXP}(E7 + E8 \times p + E9 \times p^2)/i) \end{aligned}$	(5)
Mass balance		
H ₂ production rate	$n_{\text{H}_2, \text{product}} = n_F \times \frac{I}{Z \times F} \times N$	(6)
	$n_{\text{H}_2, \text{cat}} = n_{\text{H}_2, \text{prod}}$	(7)
	$n_{\text{O}_2, \text{an}} = n_{\text{O}_2, \text{prod}} = \frac{1}{2} n_{\text{H}_2, \text{prod}}$	(8)
	$n_{\text{H}_2\text{O}} = n_{\text{H}_2, \text{prod}}$	(9)
Energy balance		
	$\Delta H = \Delta G + T\Delta S$	(10)
Thermoneutral cell voltage	$V_{\text{tn}} = \frac{\Delta H}{Z \times F}$	(11)
Heat generation in cell	$Q_{\text{gen}} = N \times I \times (V_{\text{cell}} - V_{\text{tn}})$	(12)
	$Q_{\text{excess}} = Q_{\text{gen}} - Q_{\text{loss}}$	(13)
	$\eta_{\text{en}} = \frac{n_{\text{H}_2} \times \text{LHV}_{\text{H}_2}}{W_{\text{net}}}$	(14)
	$n(\text{H}_2) = \frac{W(\text{Stack})}{V(\text{Cell}) \times Z \times F}$	(15)
	$W_{\text{net}} = W_{\text{stack}} + W_{\text{pump-R1}} + W_{\text{pump-R2}} + W_{\text{pump-H}_2\text{O}} + W_{\text{pump-cool}} + W_{\text{fan}}$	(16)
Stack power	$W(\text{stack}) = V(\text{Cell}) \times N \times I$	(17)
	$W_{\text{stack}} = V_{\text{stack}} \times I = (V_{\text{cell}} \times N) \times (i \times A_{\text{cell}})$	(18)
Fractional conversion of H ₂ O	$\text{FCW} = \frac{\text{molar mass of H}_2\text{O} \times \text{H}_2\text{O conversion}}{\text{Fraction of H}_2\text{O} \times \text{H}_2\text{O flow rate}}$	(19)

The cell voltage is a crucial parameter for analysing the performance of AEL and is calculated using Equation (2), originally developed by Ulleberg, 2003 [26]. The hydrogen production rate depends on the electrochemical performance of the cell, which is calculated using Equations (6)–(9). The total energy demand for the production of hydrogen is shown in Equation (10).

2.2. Technoeconomic Analysis for Hydrogen Generation, Compression and Storage

Considering the Australian context, this study conducted a technoeconomic analysis of hydrogen generation, compression and storage. Some of the key aspects and assumptions made for the technoeconomic analysis include the following and are also shown in Table 3:

- The capital cost of the current electrolyser is collected from Refs. [27,28], while the future price is based on the CSIRO report in Ref. [29].
- The levelised cost of hydrogen (LCH₂) production was evaluated/predicted for 2023, 2030, 2040 and 2050.
- The LCH₂ was predicted considering different electricity sources such as grid, standalone solar photovoltaic (PV), standalone wind, and a mix of solar PV and wind. The capacity factors for solar PV and wind were based on the AEMO estimates/projections [28].
- Tube trailer/truck was considered to be the mode of compressed hydrogen delivery.

- For techno-economic modelling, a 10 MW AEL electrolyser was chosen for hydrogen production. Analysis was carried out under different electricity prices, capacity factors and efficiencies to assess the economics of hydrogen production.
- Unless otherwise stated, all costs reported in the report are in 2023 US dollars (2023 USD).

Table 3. Key assumptions for electrolyser capital and operating cost [27,30–32].

Input	Units/Note	2023	2030	2040	2050
Electrolyser Parameters					
Efficiency	%	61.73%	70%	73%	76%
Electricity Consumption (kWh)	kWh/kg	54.00	52.00	50.00	48.00
Water Consumption	L/kgH ₂	10	9	9	9
Capacity Factor	%	0–100	0–100	0–100	0–100
Lifetime Stack High	hours	80,000	80,000	100,000	120,000
Degradation rate	%	1.0	1.0	1.0	1.0
Electrolyser CAPEX					
Capacity	MW	10	10	10	10
Equipment cost	USD/kW	1400	850 [33]	700 [33]	300 [29]
Total Direct Cost		18,000,000	7,000,000	5,130,000	4,410,000
Construction and Site Engineering Service	19% of direct cost	3,410,000	1,330,000	975,000	838,000
Project Contingency	1%	180,000	70,000	51,300	44,100
Total Indirect Cost	10–15%	1,800,000	700,000	513,000	441,000
Total CAPEX		23,300,000	9,100,000	6,670,000	5,730,000
Electrolyser OPEX					
Electricity Source	Optional list	Wind power	Wind power	Wind power	Wind power
Electricity price					
Water Type	Optional list	Desalinated water	Desalinated water	Desalinated water	Desalinated water
Water Cost	USD/L	0.0050	0.0050	0.0050	0.0050
O&M Cost	(%) of CAPEX	2.5	2.5	2.5	2.5
Stack Substitution	(%) of CAPEX	20	20	20	20

This study analysed the cost of hydrogen generation, transportation and storage under different scenarios and timelines. For example, hydrogen production cost in Australia was determined based on the variability of wind, solar and grid electricity prices. Moreover, we evaluated the cost of hydrogen production in Australia for 2023, 2030, 2040 and 2050. The following sections describe various costs associated with the levelised cost of hydrogen.

2.2.1. Evaluation of Levelised Cost of Hydrogen under Different Scenarios

This study modelled current and future hydrogen costs using an AEL electrolyser considering the base and best cases for the grid and renewable electricity price. The grid electricity price for 2022, 2030, 2040 and 2050 was sourced from the projection presented in the CSIRO report [34]. However, for the cash flow (upfront CAPEX, fixed operation and maintenance (FO&M) and ongoing CAPEX and water cost) and levelised cost analysis, the electricity price in the intermediate years was determined by linear interpolation. The solar and wind electricity prices were collected from the CSIRO projection for 2022, 2030, 2040 and 2050, reported in Ref. [29]. The same approach as that for grid electricity was applied to determine the electricity price for the intermediate years.

The levelised cost of hydrogen (LCH₂) is a useful indicator for the economic viability of hydrogen production and was determined using the following formula [31]:

$$LCH_2 \left(\frac{\$}{\text{kgH}_2} \right) = \frac{CAPEX \times C_r \times OPEX}{P_r \times 8760 \times C_f} \quad (20)$$

where

$CAPEX$ = Capital expenditure;
 C_r = Capital recovery factor;
 $OPEX$ = Operating expenditure;
 P_r = Hydrogen production rate (kg/y);
 C_f = Capacity factor.

2.2.2. Technoeconomic Analysis for the Compression of Hydrogen

The levelised cost of hydrogen for compression is capital cost plus energy- and non-energy-related operating cost. The following formula was used to determine the simplified levelised cost of hydrogen compression [31].

$$LCH_{2,com} \left(\frac{\$}{KgH_2} \right) = CAPEX_{com} \left(\frac{\$}{KgH_2} \right) + \frac{\text{Energy OPEX}_{comp} \left(\frac{\$}{KgH_2} \right) + \text{Non - energy OPEX}_{comp} \left(\frac{\$USD}{KgH_2} \right)}{P_r \times C_f} \quad (21)$$

The assumption for the modelling of $LCH_{2,com}$ is reported in Table 4. The capital cost for the compression was calculated based on Equation (22). Here, the design capacity determines the amount of hydrogen that can be compressed throughout the year. The capacity factor or availability of a compressor is generally assumed to be 90%, meaning an outage of 10% of the time in a year.

$$CAPEXH_{2,com} \left(\frac{\$}{KgH_2} \right) = \frac{\text{Annualised TCI} \left(\frac{\$}{yr} \right)}{\text{Design capacity} \left(\frac{kgH_2}{day} \right) \times 365 \times \text{Capacity factor}(\%)} \quad (22)$$

where

$$\text{Annualised TCI} \left(\frac{\$}{yr} \right) = \text{TCI} \times \text{CRF} \quad (23)$$

where TCI = total capital investment (USD), calculated based on

$$\text{TCI} = \text{TIC} \times \text{indirect cost} \quad (24)$$

where TIC is the total installation cost, calculated based on the following equation:

$$\text{TIC} = \text{Compressor cost} \times \text{Installation factor (IF)} \quad (25)$$

CRF is the capital recovery rate which is calculated based on the following equation.

$$\text{CRF} = \frac{i(1+i)^n}{(1+i)^n - 1} \quad (i = \text{discount rate, \%, and } n = \text{compressor lifetime}) \quad (26)$$

In this modelling, the indirect cost was assumed to be 40% of the total installation cost, which considered the following parameters: site preparation = 5% of TIC, engineering and design = 10% of TIC, project contingency = 10% of TIC, permitting = 3% of TIC and owner's costs = 12% of TIC [35]. The operating cost is composed of energy- and non-energy-related costs.

Energy-related operating cost was calculated based on the following equation:

$$\text{Energy OPEX}_{comp} \left(\frac{\$}{KgH_2} \right) = \frac{\text{Electricity cost} \left(\frac{\$}{yr} \right)}{\text{Design capacity} \left(\frac{kgH_2}{day} \right) \times 365 \times \text{Capacity factor}(\%)} \quad (27)$$

On the other hand, non-energy-related operating cost was calculated based on the following equation:

$$\text{Non – energy OPEX}_{\text{comp}} \left(\frac{\$}{\text{KgH}_2} \right) = \frac{\text{Non – energy OPEX} \left(\frac{\$}{\text{yr}} \right)}{\text{Design capacity} \left(\frac{\text{kgH}_2}{\text{day}} \right) \times 365 \times \text{Capacity factor}(\%)} \quad (28)$$

$$\text{Non – energy OPEX} = \text{Total labour cost} \left(\frac{\$}{\text{yr}} \right) + \text{Fixed O\&M} \left(\frac{\$}{\text{yr}} \right) \quad (29)$$

Hence,

$$\text{Total labour cost} \left(\frac{\$}{\text{yr}} \right) = \text{Direct labour} \left(\frac{\$}{\text{yr}} \right) + \text{Indirect labour} \left(\frac{\$}{\text{yr}} \right) \quad (30)$$

$$\text{Direct labour} \left(\frac{\$}{\text{yr}} \right) = \text{Annual hour}(\text{h/yr}) \times \text{Labour rate}(\$/\text{h}) \quad (31)$$

$$\text{Annual labour hour} \left(\frac{\text{h}}{\text{yr}} \right) = 288 \times \left(\frac{\text{Compressor flow rate}(\text{kgH}_2/\text{day})}{100,000} \right)^{0.25} \quad (32)$$

$$\text{Indirect labour} \left(\frac{\$}{\text{yr}} \right) = \text{Direct labour} \left(\frac{\$}{\text{yr}} \right) \times \text{Indirect labour factor}(\%) \quad (33)$$

Finally, fixed operations and maintenance (O&M) costs were calculated considering operating, maintenance and repairs = 4% of TIC; insurance = 1% of TCI; property tax = 1% of TCI; and licensing and permitting = 0.1% of TCI.

Table 4. Detailed economic assumptions for the calculation of LCH₂ for compression.

Factor	Value	Comment and Ref.
Inflation rate	2–4%	[36,37]
Discount rate	8%	Discount rate = weighted average cost of capital (WACC)
Project lifetime	25 years	Assumed [35]
Electricity cost	0.8 USD/kWh	[34,38]
Capacity factor	95%	Assumed [35]
Scaling factor	0.83	Assumed [35]
Installation factor	2	Assumed [35]
Compressor cost	CC [2022 USD] = 3083.3 × (P _{rated}) ^{SF} , where scale factor (SF) = 0.8335	The data were retrieved from [35] and converted into 2023 USD using the inflation rate provided in Ref. [36]
Labour rate	75.5 USD/h	Ref. [39]
Indirect labour factor	50%	Ref. [35]

3. Results and Discussion

3.1. Mathematical Modelling of AEL

The performance parameters of the electrolyser, such as stack power, cell voltage, heat generation, hydrogen production and the diffusion of hydrogen to oxygen (HTO), are shown in Figure 1a concerning current density and stack temperature. Increasing the current density increases stack voltage and corresponding power progressively. The stack voltage is recorded as 21.4 to 27.20 V at a temperature of 50 °C using the current density of 0.1 to 0.6 A/cm². However, increasing temperature decreases the stack voltage steadily. For instance, using the current density of 0.1 A/cm², the stack voltage decreases from 21.4 to 19.3 V when the temperature is increased from 50 to 90 °C. As a result, with increasing temperature, the stack power demand in the electrolyser decreases [10]. At 50 °C, stack power is found to be 2.14 to 16.32 W over the current densities. Over the

temperature range (50 to 90 °C), the stack power decreases by 0.21 to 1.3 W for the current density of 0.1 to 0.6 A/cm².

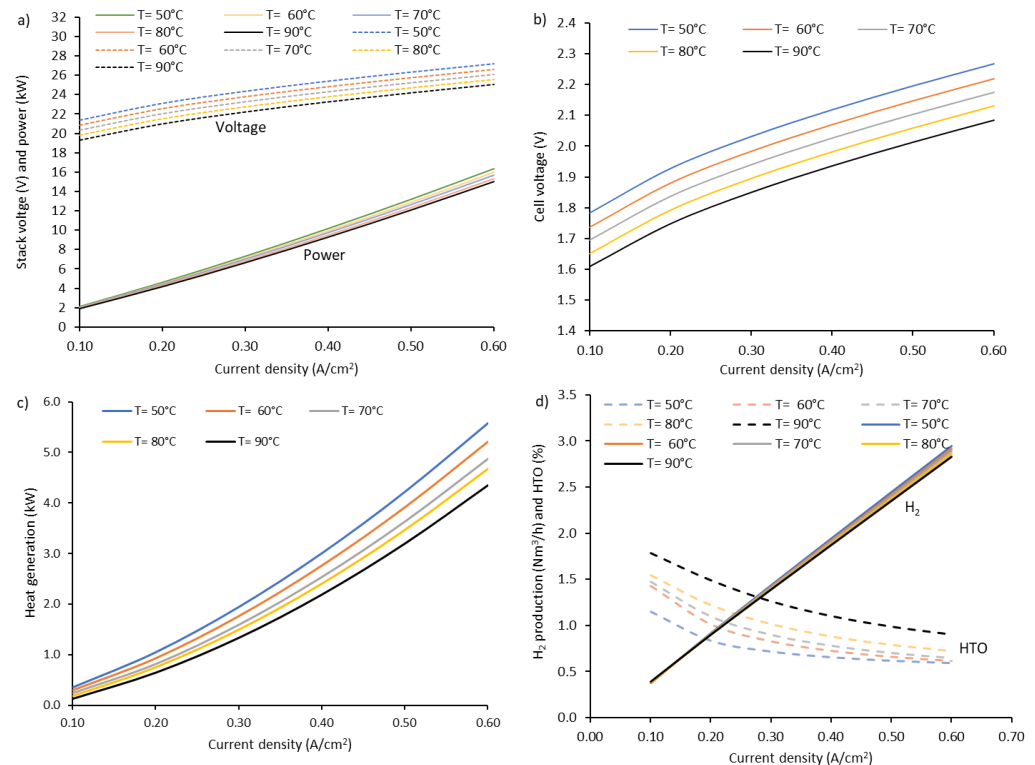


Figure 1. Effect of temperature on (a) stack power, (b) cell voltage, (c) heat generation and (d) hydrogen production and content of H₂ in oxygen (HTO).

The effect of current density on cell voltage is shown in Figure 1b. Increasing the current density increases the cell voltage [10]. However, an opposite trend with increasing temperature is observed. The cell voltage is found to be 1.78 to 2.27 at 50 °C and decreases to 1.61 to 2.09 at 90 °C. The heat generated in the stack increases exponentially with increasing current density [10]. Similar to cell voltage and stack power, increasing temperature decreases the heat generation primarily due to activation overpotential, as shown in Figure 1c. Heat generation is recorded to be 0.29 to 5.22 kW over the current density at 50 °C and decreases to 0.12 to 4.35 kW at 90 °C.

The effect of temperature on hydrogen production and the content of H₂ in oxygen (HTO) is shown in Figure 1d. As can be seen, increasing current density increases hydrogen production. However, overall, increasing the temperature decreases hydrogen production [10]. This result is attributed to the fact that increasing temperature decreases the resistance, resulting in increasing parasitic loss and thus lowering Faradic efficiency [26]. The maximum H₂ production at 0.6 A/cm² is recorded to be 2.94 Nm³/h at 50 °C and decreases to 2.83 Nm³/h at 90 °C. Increasing current density exponentially decreases the quantity of hydrogen in the oxygen, but increasing temperature increases the HTO, producing more impurities at higher temperatures [11]. With increasing temperature, impurities increase due to diffusion phenomena and gas migration [10]. At 50 °C, An HTO of 1.15 to 0.6 was recorded over the current densities, and the HTO increased by 0.64 to 0.31%-point when the temperature was increased to 90 °C over the current densities. Noticeably, the content of hydrogen in oxygen is higher at lower current density due to the lower gas production [11,40]. Hence, an electrolysis system needs to maintain an optimum current density balancing with heat loss and purity to ensure safety standards [40].

The effect of pressure (bar) on the performance of the alkaline electrolyser at a constant temperature of 75 °C is shown in Figure 2. Pressure is found to have minimal effect on all

performance parameters. For example, the cell voltage is recorded to be 1.67 to 2.15 V at 5 bar, increasing slightly to 1.67 to 2.17 when the pressure is increased to 13 bar (Figure 2a). The trend is found to be opposite to that of temperature. Stack voltage increases with increasing pressure negligibly with an average voltage of 20–26 V over the current density of 0.1 to 0.6 A/cm². However, the stack power is recorded to be 2.0 to 15.55 kW on average—increasing pressure increases the power insignificantly (Figure 2b). The average heat generation concerning current density is 0.2 to 4.75 kW (Figure 2c). Production of hydrogen concerning pressure has no effect with 0.38 to 2.87 Nm³/h over the current density (Figure 2d). An exponential decay for HTO concerning current density is found with significantly higher impurities or HTO using pressure over 11 bar, because increasing pressure increases the solubility of gas in the electrolyte and diffusion of gases between the electrolytic cells [10].

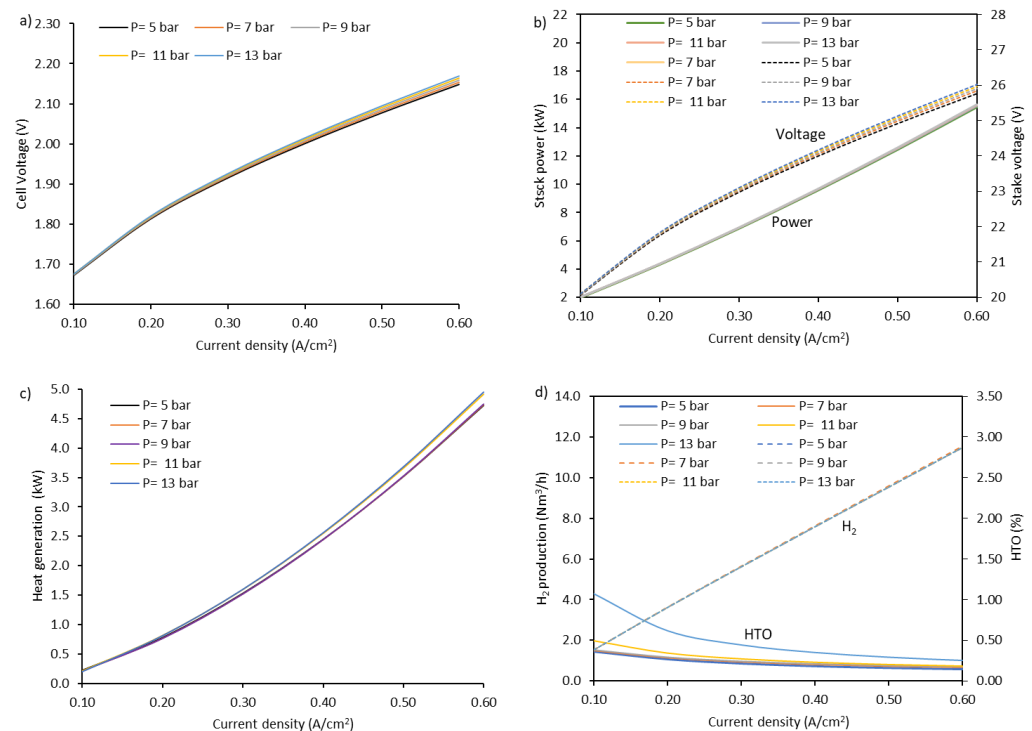


Figure 2. Effect of pressure on (a) stack power, (b) cell voltage, (c) heat generation and (d) hydrogen production and the content of H₂ in oxygen (HTO).

3.2. Technoeconomic Analysis Results

Levelised Cost of Hydrogen

The current LCH₂ using grid electricity was calculated to be USD 5.0, which increases to just over USD 6.0 and USD 7.0 in 2030 and 2040, respectively, assuming a capacity factor of 95%, as shown in Figure 3a. As expected, the major contributor in LCH₂ is electricity (70.8%), followed by upfront CAPEX (20.8%), fixed operation and maintenance (FO&M) (5.8%), ongoing CAPEX (1.7%) and water (0.9%). The upfront CAPEX and electricity cost can be summed to 92%. The cost of grid electricity is forecasted to increase in the coming years, with a prediction of about 43% and 75% in 2030 and 2040, respectively, because of the cheaper renewables and government policies [41]. However, the cost of other aspects will decrease, especially upfront CAPEX and FO&M.

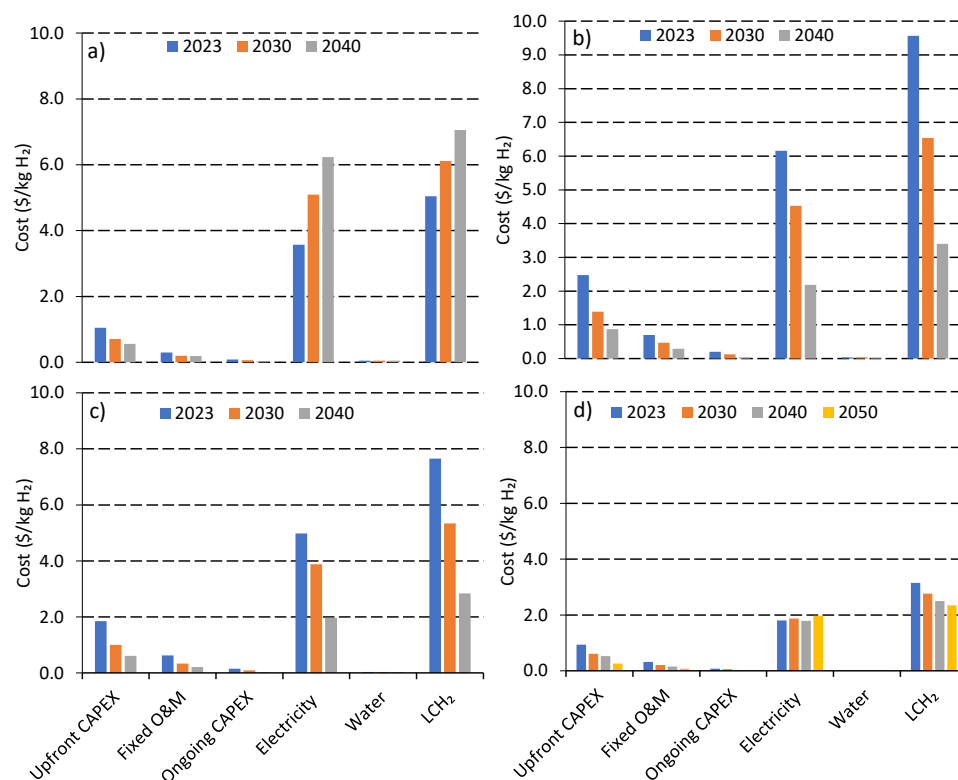


Figure 3. Current and projected cost of hydrogen production using AEL assuming base case for electricity price: (a) grid, (b) standalone solar, (c) standalone wind and (d) solar and wind mix.

The LCH₂ using electricity from standalone solar PV is shown in Figure 3b. The LCH₂ in 2023 is calculated to be USD 9.6 using a base-case solar electricity price of 65–38 USD/MWh in contrast to grid electricity price of 67–155 USD/MWh over the cash flow period of 2023–2053. Noticeably, the higher LCH₂ using electricity from standalone solar PV is primarily due to the lower capacity factor of about 0.30. Thus, using solar AEL, the total hydrogen production over the period is predicted to be 68% lower than that for grid-based AEL, which leads to an increase in all other costs in cash flow. The contribution of solar electricity (65%) in current LCH₂ is 6.0%-point lower than that of grid electricity (71%). However, the upfront CAPEX, FO&M and ongoing CAPEX using solar electricity are 6%, 1.5% and 0.4%-point higher than grid electricity. A sharp decline in upfront CAPEX, solar electricity and overall LCH₂ is expected by 2030. As seen, the LCH₂ is expected to be USD 6.5 and USD 3.4 by 2030 and 2040. The LCH₂ using solar power varies significantly depending on the geographical location. For example, considering the European context, Lee et al., 2023 [22] reported an optimum LCH₂ of 12.86 USD/kgH₂ using concentrated solar power, while Ibagon et al., 2023 [24] reported a much lower LCH₂ with 3.5 USD/kgH₂ considering the South American country Uruguay because the cost of solar electricity and the capacity factor vary significantly with respect to geographical location [24].

Moreover, cost reduction (LCH₂) using wind is more promising. The predicted LCH₂ using electricity from standalone wind energy is shown in Figure 3c. The current LCH₂ using wind is determined to be about USD 7.7 using a base-case electricity price of 57–52 USD/MWh over the cash flow period of 2023–2053 compared to the forecasted solar electricity price of 65–38 USD/MWh. The current LCH₂ using wind is USD 1.9 lower than that for solar-based electricity.

Despite higher electricity prices, the lower LCH₂ using standalone wind is primarily due to the higher capacity factor of about 0.40–0.46 over the cash flow period of 2023 to 2053. Thus, using wind-based standalone AEL, the total hydrogen production over the period is calculated to be 20% higher than that for solar-based AEL, leading to a decrease in the LCH₂. Despite the lower cost, the cost contribution in CAPEX, FO&M and ongoing CAPEX from

current wind-based LCH₂ is roughly similar to that of standalone solar. As in the case of standalone solar, a sharp decline in upfront CAPEX, electricity and overall LCH₂ is expected using wind-based electricity in the coming decades. Babarit et al., 2018 [23] reported an LCH₂ of about 10–14 USD/kgH₂ using the current offshore wind-based electricity price of USD 0.12/kWh. The LCH₂ using standalone wind electricity is calculated to be USD 5.3 and USD 2.9 in 2030 and 2040, as shown in Figure 3c.

A remarkable decrease in cash flow parameters and overall LCH₂ is predicted using a solar and wind mix (SWM), as shown in Figure 3d. Currently, the LCH₂ using SWM is estimated to be USD 3.2 compared to USD 9.6 and USD 7.7 using standalone solar and wind. This cost is expected to decrease further in the coming decades, with an estimated LCH₂ at USD 2.7, USD 2.5 and USD 2.4 in 2030, 2040 and 2050, respectively. This decrease in LCH₂ using SWM is primarily due to the increase in the capacity factor by at least 33%.

In contrast, considering the best-case renewable electricity price, the scenario changes substantially regarding current and future cash flow parameters and LCH₂. The best-case solar and wind electricity price is projected to be 44 to 18 USD/MWh and 45 to 30 USD/MWh, compared to 65 to 38 USD/MWh and 57 to 52 USD/MWh under the base case over the cash flow period of 2023 to 2053. Under the best-case scenario, the current LCH₂ using standalone solar is calculated to be USD 5.7, which is USD 3.9 lower than that under the base case, as shown in Figure 4a. Likewise, in the base case, the cash flow parameters and LCH₂ under the best case are forecasted to decrease sharply in the coming decades. For instance, LCH₂ under the best case is predicted to be USD 3.9 and USD 2.1 compared to USD 6.5 and USD 3.4 under base-case solar PV in 2030 and 2040, respectively.

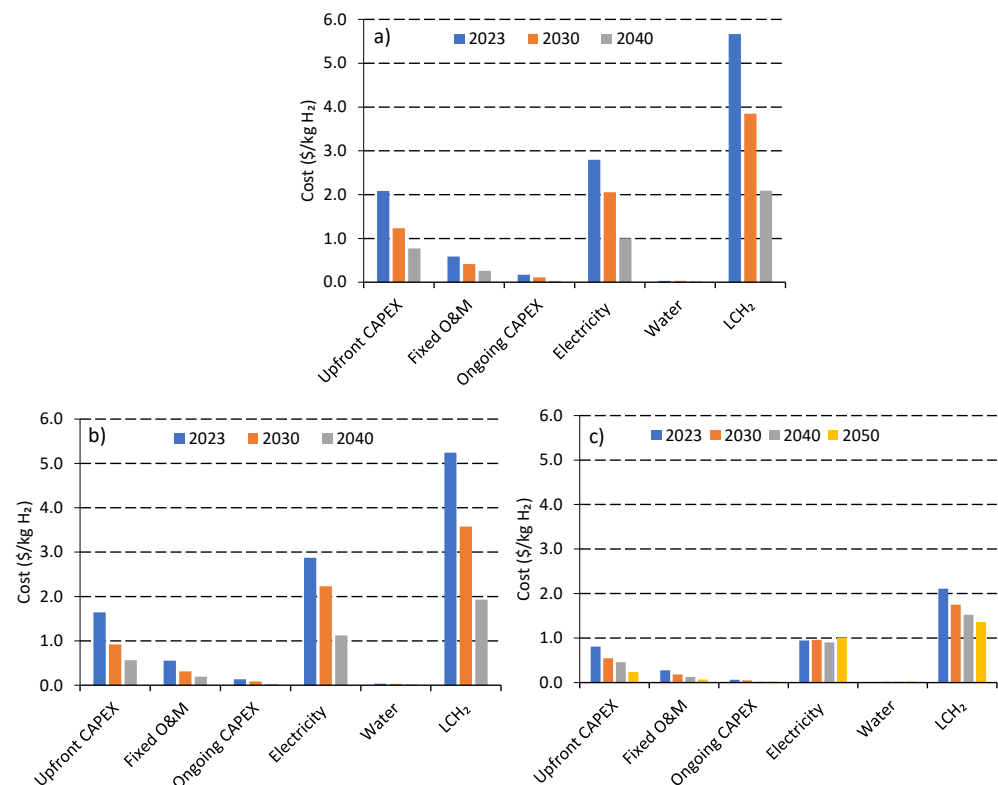


Figure 4. Current and projected cost of hydrogen production under best-case electricity price: (a) standalone solar, (b) standalone wind and (c) solar and wind mix.

Furthermore, according to Figure 4b, the current and future LCH₂ values using standalone wind are predicted to be about 7–8% lower than those using standalone solar. Moreover, considering best-case SWM, a drastic decrease in current and future LCH₂ is determined. As shown in Figure 4c, using the best-case SWM, the current LCH₂ is ~USD 2.1,

decreasing to USD 1.7, USD 1.5 and USD 1.4 in 2030, 2040 and 2050. Hence, using SWM, compared to the base case, the best case offers 33% lower LCH₂ in 2023, which leads to 37, 39 and 42% in 2030, 2040 and 2050, respectively.

The following section describes the cost of hydrogen compression, transportation and storage. These studies are particularly important if industries want to source hydrogen from a hydrogen generation plant instead of onsite generation. Hence, knowing the entire cost breakdown associated with hydrogen and its implications is important.

3.3. Compressor Power Calculation

Followed by the cost of production, hydrogen compression dominates the delivery cost in the hydrogen supply chain [42]. Thus, some basic calculations to understand the energy, capital expenditure, operating cost and levelised cost for compression are reported in this section. A single-stage compressor was designed with a capacity of 123,196 Nm³H₂/h (10.96 tH₂/h) using solar and wind farms, assuming a design capacity of 600 MW with a capacity factor of 0.3 and 0.45, respectively. The process flow diagram for H₂ compression is shown in Figure 5.

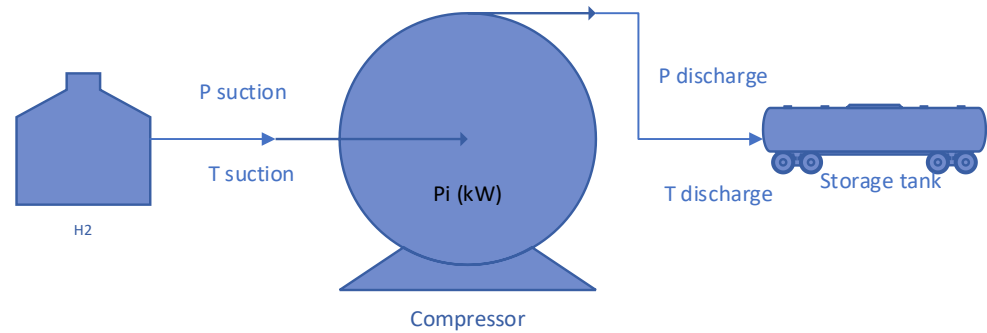


Figure 5. Process flow diagram for hydrogen compression.

In modelling, the suction pressure and temperature of the compressor are assumed to be 20 bar and 75 °C, respectively, while the efficiency of the compressor is assumed to be 85%. Moreover, the detailed formulas and assumptions used for the modelling are reported in Table 2. The required isentropic power for the single-stage reciprocating compressor is designed at various compression ratios or discharge pressure according to the following equations [35].

$$P_i = 2.31 \frac{k}{(k-1)} \times \frac{(T_{dis} - T_{suct})}{M} \times Q_m \quad (34)$$

P_i = Power (kW);

T_{suct} = Compressor inlet temperature (K);

T_{dis} = Compressor outlet temperature (K);

M = Molar weight of the hydrogen gas (g/mol);

Q_m = Compressor throughput (kg/h);

k = Isentropic coefficient of the gas (1.4).

The discharge temperature of the compressor was calculated using the following formula:

$$\frac{T_{out}}{T_{in}} = \left(\frac{p_2}{p_1} \right)^{\frac{(\gamma-1)}{\gamma}} \quad \left(\gamma = \frac{C_p}{C_v} \right) \quad (35)$$

The effect of the compression ratio (outlet to the inlet pressure of the gas) on compressor power and discharge temperature is shown in Figure 6. The study considered the discharge pressure of 30 to 700 bar, leading to a compression ratio of 1.5 to 35. As an obvious fact, increasing compression ratio (CR) increases the power required and discharge temperature of the compressor following a logarithmic trend. Generally, the tube trailer is filled with pressure over 350 bar. Results show that a tube trailer with a pressure of

350 bar (CR = 17.5) requires a compressor with a power of 22.8 MW, while a compressor power of 32 MW is required when doubling the tube pressure. Increasing the compression ratio leads to an increase in the discharge temperature. For example, at a CR of 17.5, the discharge temperature is 789 K compared to 962 K using a CR of 35.

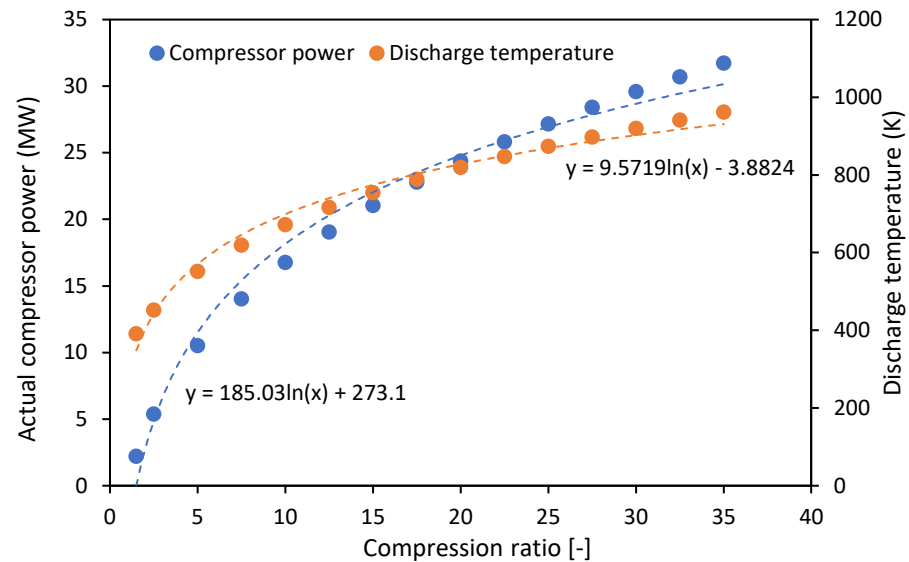


Figure 6. Effect of compression ratio on compressor power and discharge temperature.

The energy consumption for hydrogen compression concerning the compression ratio is shown in Figure 7. This figure also shows the percentage of energy required from hydrogen itself for compression. Increasing the compression ratio increases energy consumption, as does hydrogen energy. Noticeably, the increase in energy consumption at lower CR is faster than that at higher CR. As can be seen, compression of H₂ with a compression ratio between 1.5 and 35 leads to the consumption of energy with a range of 0.25 to 3.4 kWh/kgH₂, which is equivalent to 0.70 to 10% of the energy from H₂ considering a lower heating value, compared to 40% loss of energy for making liquid hydrogen [43].

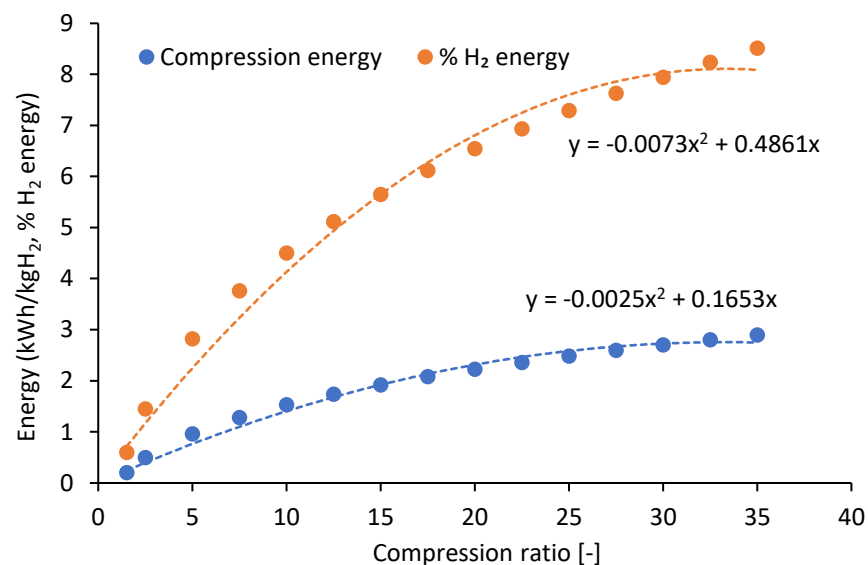


Figure 7. Consumption of hydrogen concerning compression ratio.

3.4. Technoeconomic Analysis for the Compression of Hydrogen

An important indicator regarding the economic viability of any financial investment in a project is the levelised cost. This section describes the simplified levelised cost of hydrogen for compression, a technique of processing hydrogen among different physicochemical forms [44]. The formula and assumptions used to derive levelised cost are reported in Section 2.2.2.

The initial design is carried out for a hydrogen flow rate of 10,964 kg/h (263 tonnes/day), similar to designing compressor power requirements. After that, a sensitivity study is carried out for capacities ranging from 5 to 300 tonnes/day H_2 . The total capital cost concerning design capacity is shown in Figure 8a. The CAPEX increases with increasing design capacity. However, the cost is lower when the design capacity is higher. For example, the CAPEX is 0.15 million USD/t H_2 while designing 5.0 t/day H_2 , leading to half of 0.075/t H_2 in the case of 300 t/day H_2 .

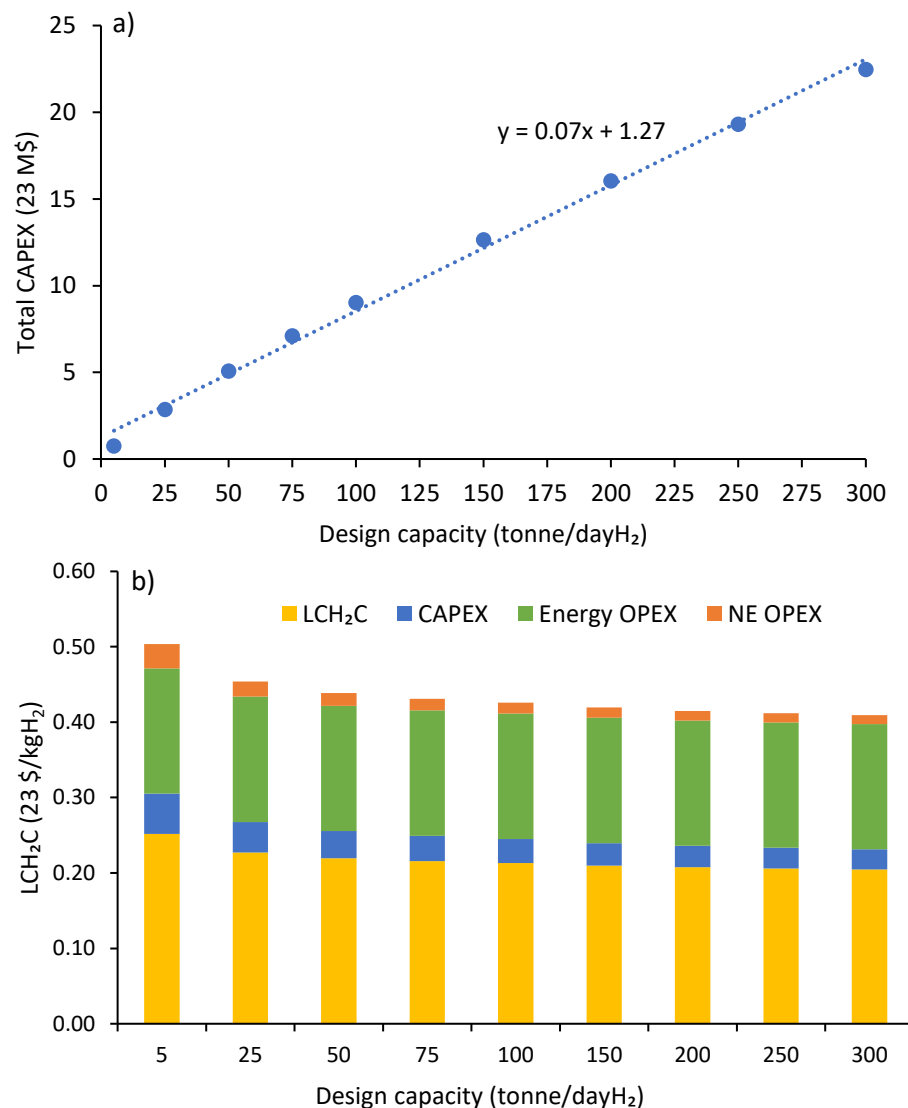


Figure 8. (a) Total capital cost and (b) levelised cost for the compression of hydrogen concerning design capacity.

The variation in the levelised cost of compression (LCH $_2$ C) is shown in Figure 8b. The LCH $_2$ C nearly follows an exponential decay trend concerning design capacity. For example, for a design capacity of 5.0 tonnes/day, the LCH $_2$ C is USD 0.25, which decreases to

USD 0.20 for 300 tonnes/day capacity, similar to the cost reported by Ibagon et al., 2023 [24]. The changes seem insignificant, particularly with a capacity above 75 tonnes/day. The major contributor in LCH₂C is energy-related operating cost, which is a constant value of USD 0.16, followed by the CAPEX for the compressor (USD 0.053–USD 0.027) and non-energy-related OPEX (USD 0.032–USD 0.012). The latter two parameters decrease with increasing design capacity. According to Ibagon et al., 2023 [24], the levelised cost of processing/compression is about 2.5–3% of the levelised cost of production in 2022. According to the current study, considering the best-case wind- and solar-based hydrogen, the current levelised cost of hydrogen compression is about 4–5% of the levelised for hydrogen production (Figure 4).

3.5. Technoeconomic Analysis for the Transportation of Hydrogen

The levelised cost of hydrogen for transportation concerning round-trip travel distance, the operating pressure of the tube trailer and design capacity is shown in Figure 9. As can be observed, the levelised cost of hydrogen transportation (LCH₂T) concerning travel distance decreases with increasing round-trip distance. The LCH₂T comprises the cost of the tractor and tube trailer. The tractor costs include capital investment, labour, fuel and fixed operating and maintenance costs. In contrast, the cost associated with tube trailers primarily includes capital investment, operating and maintenance costs. Over the range of travel distance of 300–1000 km, the tractor cost varies from USD 0.68 to USD 0.61/kg while the cost for a tube trailer is almost constant at 0.39, as shown in Figure 9a. Hence, the total cost with regard to the travel distance is over the range of USD 1.07 to USD 1.01/kg, which is similar to the cost reported by Ibagon et al., 2023 [24].

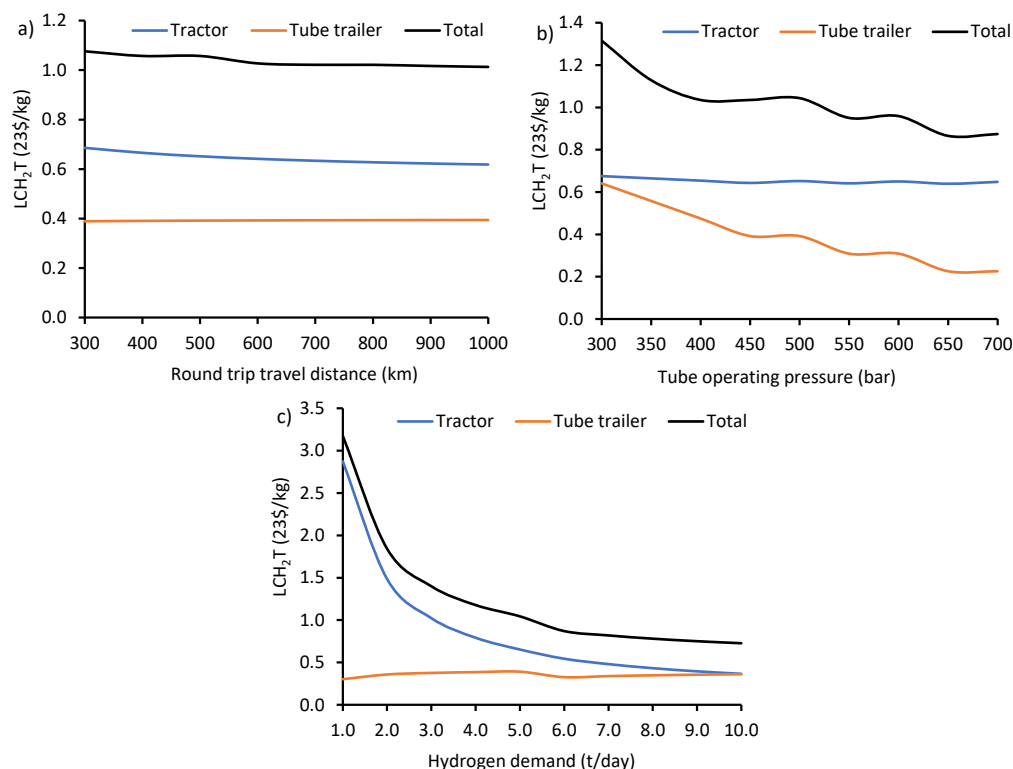


Figure 9. Levelised cost of hydrogen for transportation concerning (a) round-trip travel distance with a constant pressure of 500 bar and hydrogen demand of 5 t/day, (b) operating pressure with a constant distance of 500 km and hydrogen demand of 5 t/day, and (c) hydrogen demand with a constant distance of 500 km and pressure of 500 bar.

Likewise, the levelised cost of transportation decreases markedly with increasing operating pressure, as shown in Figure 9b. Increasing operating pressure from 300 to 600 bar

decreases the cost by 46%, and the cost ranges from 1.5 to 0.81 USD/kgH₂. As can be seen, like travel distance, operating pressure has an insignificant effect in terms of the tractor cost, which varies from 0.67 to 0.64 USD/kgH₂ over the range. However, the tube trailer has a marked impact on LCH₂T concerning operating pressure, and the LCH₂T varies from 0.64 to 0.22 USD/kgH₂ over the range. Thus, the total LCH₂T comprising a tractor and tube trailer is 1.31 to 0.87 USD/kgH₂ over the operating pressure of 300 to 700 bar.

Furthermore, increasing design capacity from 1 to 10 tonnes/day decreases the total LCH₂T by 77%, and the LCH₂T ranges from 3.17 to 0.72 USD/kgH₂ (Figure 9c). Unlike the other two cases, the tractor significantly impacts LCH₂T with respect to design capacity, while the impact of the tube trailer is minimal. Overall, it is found that to keep the LCH₂T low, the tube operating pressure and design capacity should be as high as possible.

It is noteworthy to mention that, in the case of pipeline transportation, an existing natural gas pipeline may not be compatible with hydrogen. Moreover, valves, fittings and other piping-related instruments must be modified. Hence, a significant capital investment might be required in this aspect for the application of hydrogen in industries.

3.6. Technoeconomic Modelling for the Storage of Hydrogen

The levelised cost of storage, CAPEX and OPEX for the geological storage of hydrogen concerning the average hydrogen flow rate is shown in Figure 10. The LCH₂ for storage decreases following an exponential decay trend with increasing to average hydrogen flow rate. The LCH₂ for storage using the design capacity of 5 tonnes/day (0.6 million m³) costs 0.29 USD/kgH₂ which decreases to 0.15 USD/kgH₂ for the design capacity of 20 tonnes/day (2.42 million Nm³) following the power law of $y = 0.58x^{-0.44}$, where y represents the LCH₂ for storage and x represents the average hydrogen flow rate. A similar cost related to the storage of hydrogen was reported by Ibagon et al., 2023 [24].

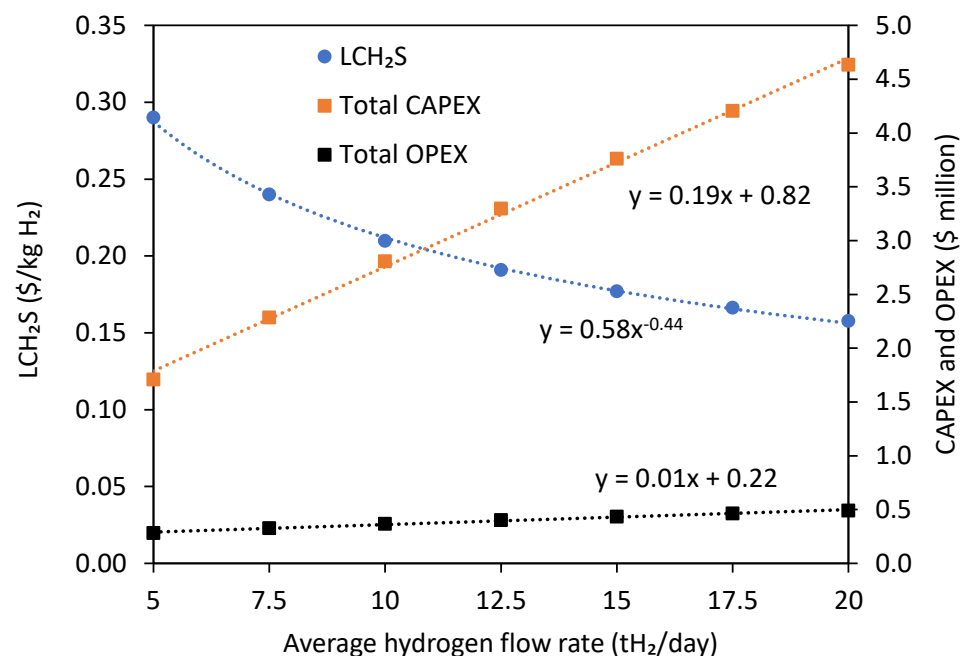


Figure 10. LCH₂ for storage, CAPEX and OPEX for the geological storage of hydrogen concerning design capacity of 45 tonnes and hydrogen leaving pressure of 70 bar.

The capital cost increases linearly with respect to the average hydrogen flow rate, ranging from USD 1.7 to USD 4.63 million, following a linear relationship of $y = 0.19x + 0.82$, where y represents the CAPEX for storage and x represents the average hydrogen flow rate. The OPEX for the geological storage is found to be USD 0.28 million with an average hydrogen flow rate of 5.0 tonnes/day and increases to USD 0.5 million when the average

hydrogen flow rate is increased to 20 tonnes/day. Regardless of onsite generation or external sourcing, a process or manufacturing industry needs to construct storage facilities and store hydrogen equivalent to the plant's demand for a few days.

4. Conclusions

In terms of the performance of an alkaline electrolyser, the modelling results show that an increase in the current density progressively increases the cell voltage, stack voltage and corresponding power and ultimately increases the hydrogen production. However, increasing current density increases heat loss and safety concerns. On the other hand, increasing the temperature was predicted to decrease the cell voltage, stack voltage, stack power and hydrogen production. Increasing the current density was predicted to decrease the hydrogen concentration in oxygen exponentially. In contrast, pressure was found to have minimal effect on all performance parameters at a constant temperature.

Technoeconomic modelling for hydrogen generation shows that electricity is the key factor for green hydrogen generation with a current cost of 7.7 to 9.6 USD/kgH₂ using wind and solar under the base case. The higher levelised cost using standalone solar PV is primarily due to the lower capacity factor of about 0.30 compared to over 0.4 using wind-based electricity. Currently, 71% of the cost of hydrogen is due to the use of electricity, followed by upfront CAPEX of 20%, and the remaining 9% is due to the fixed operating and maintenance, ongoing CAPEX and water. The cost contribution of hydrogen using PV electricity is 14%-point lower than that of grid electricity. However, the upfront CAPEX, FO&M and ongoing CAPEX using solar electricity are 6%, 1.5% and 0.4%-point higher than those using grid electricity.

A sharp decline in upfront CAPEX, solar electricity and the overall cost of hydrogen is expected in the coming decades, with an estimated 6.5 and 3.4 USD/kgH₂ by 2030 and 2040. A further reduction with standalone wind is expected with 5.3 and 2.9 USD/kgH₂ by 2030 and 2040, respectively. The current levelised cost using a solar and wind mix (SWM) is estimated at 3.2 USD/kgH₂ compared to USD 9.6 and USD 7.7 using standalone solar and wind. This SWM cost is expected to decrease in the coming decades with an estimated 2.7, 2.5 and 2.4 USD/kgH₂ in 2030, 2040 and 2050, respectively. A decreasing hydrogen price in the coming decades means hydrogen will have widespread applications in industries and thereby a favorable impact on our environment. The current and future costs for hydrogen change substantially when considering the best-case electricity price from solar and wind. A calculation concerning compression, transportation and hydrogen storage shows that an additional USD 1.5 to USD 2.0 is required where the hydrogen demand is at least 5 tH₂/day. A comparative fundamental and technoeconomic study concerning other electrolyser technologies is recommended for future study.

Author Contributions: Conceptualization, M.S.; Methodology, M.S.; Software, M.S.; Validation, M.A.R.; Formal analysis, M.S.; Investigation, M.S.; Resources, M.A.R. and G.A.B.; Writing—original draft, M.S.; Writing—review & editing, M.S., M.A.R. and G.A.B.; Supervision, M.A.R. and G.A.B.; Project administration, M.A.R. and G.A.B.; Funding acquisition, M.A.R. and G.A.B. All authors have read and agreed to the published version of the manuscript.

Funding: This research was funded by Victorian Hydrogen Hub (VH2), Swinburne University of Technology, Australia.

Data Availability Statement: The data presented in this study are available on request from the corresponding author. The data are not publicly available due to the nature of the study.

Conflicts of Interest: The authors declare no conflict of interest.

References

1. IEA. *International Energy Agency Global Hydrogen Review 2021*; OECD Publishing: Paris, France, 2021.
2. Khojasteh Salkuyeh, Y.; Saville, B.A.; MacLean, H.L. Techno-economic analysis and life cycle assessment of hydrogen production from natural gas using current and emerging technologies. *Int. J. Hydrogen Energy* **2017**, *42*, 18894–18909. [[CrossRef](#)]
3. Shahabuddin, M.; Brooks, G.; Rhamdhani, M.A. Decarbonisation and hydrogen integration of steel industries: Recent development, challenges and technoeconomic analysis. *J. Clean. Prod.* **2023**, *395*, 136391. [[CrossRef](#)]
4. Salkuyeh, Y.K.; Saville, B.A.; MacLean, H.L. Techno-economic analysis and life cycle assessment of hydrogen production from different biomass gasification processes. *Int. J. Hydrogen Energy* **2018**, *43*, 9514–9528. [[CrossRef](#)]
5. Ali Khan, M.H.; Daiyan, R.; Neal, P.; Haque, N.; MacGill, I.; Amal, R. A framework for assessing economics of blue hydrogen production from steam methane reforming using carbon capture storage & utilisation. *Int. J. Hydrogen Energy* **2021**, *46*, 22685–22706.
6. Turner, J.; Sverdrup, G.; Mann, M.K.; Maness, P.C.; Kroposki, B.; Ghirardi, M.; Evans, R.J.; Blake, D. Renewable hydrogen production. *Int. J. Energy Res.* **2008**, *32*, 379–407. [[CrossRef](#)]
7. Kotowicz, J.; Jurczyk, M.; Węcel, D.; Ogulewicz, W. Analysis of hydrogen production in alkaline electrolyzers. *J. Power Technol.* **2016**, *96*, 149.
8. Lehner, M.; Tichler, R.; Steinmüller, H.; Koppe, M. *Power-to-Gas: Technology and Business Models*; Springer: Berlin/Heidelberg, Germany, 2014.
9. Shiva Kumar, S.; Lim, H. An overview of water electrolysis technologies for green hydrogen production. *Energy Rep.* **2022**, *8*, 13793–13813. [[CrossRef](#)]
10. Sanchez, M.; Amores, E.; Abad, D.; Rodriguez, L.; Clemente-Jul, C. Aspen Plus model of an alkaline electrolysis system for hydrogen production. *Int. J. Hydrogen Energy* **2020**, *45*, 3916–3929. [[CrossRef](#)]
11. Sánchez, M.; Amores, E.; Rodríguez, L.; Clemente-Jul, C. Semi-empirical model and experimental validation for the performance evaluation of a 15 kW alkaline water electrolyzer. *Int. J. Hydrogen Energy* **2018**, *43*, 20332–20345. [[CrossRef](#)]
12. Buttler, A.; Spliethoff, H. Current status of water electrolysis for energy storage, grid balancing and sector coupling via power-to-gas and power-to-liquids: A review. *Renew. Sustain. Energy Rev.* **2018**, *82*, 2440–2454. [[CrossRef](#)]
13. Ursua, A.; Gandia, L.M.; Sanchis, P. Hydrogen production from water electrolysis: Current status and future trends. *Proceedings IEEE* **2011**, *100*, 410–426. [[CrossRef](#)]
14. Zeng, K.; Zhang, D. Recent progress in alkaline water electrolysis for hydrogen production and applications. *Prog. Energy Combust. Sci.* **2010**, *36*, 307–326. [[CrossRef](#)]
15. Li, X.; Walsh, F.C.; Pletcher, D. Nickel based electrocatalysts for oxygen evolution in high current density, alkaline water electrolyzers. *Phys. Chem. Chem. Phys.* **2011**, *13*, 1162–1167. [[CrossRef](#)]
16. Pletcher, D.; Li, X. Prospects for alkaline zero gap water electrolyzers for hydrogen production. *Int. J. Hydrogen Energy* **2011**, *36*, 15089–15104. [[CrossRef](#)]
17. Leng, Y.; Chen, G.; Mendoza, A.J.; Tighe, T.B.; Hickner, M.A.; Wang, C.-Y. Solid-state water electrolysis with an alkaline membrane. *J. Am. Chem. Soc.* **2012**, *134*, 9054–9057. [[CrossRef](#)]
18. Zghaibeh, M.; Barhoumi, E.M.; Okonkwo, P.C.; Ben Belgacem, I.; Beitelmal, W.H.; Mansir, I.B. Analytical model for a techno-economic assessment of green hydrogen production in photovoltaic power station case study Salalah city—Oman. *Int. J. Hydrogen Energy* **2022**, *47*, 14171–14179. [[CrossRef](#)]
19. Benalcazar, P.; Komorowska, A. Prospects of green hydrogen in Poland: A techno-economic analysis using a Monte Carlo approach. *Int. J. Hydrogen Energy* **2022**, *47*, 5779–5796. [[CrossRef](#)]
20. Minutillo, M.; Perna, A.; Forcina, A.; Di Micco, S.; Jannelli, E. Analyzing the levelized cost of hydrogen in refueling stations with on-site hydrogen production via water electrolysis in the Italian scenario. *Int. J. Hydrogen Energy* **2021**, *46*, 13667–13677. [[CrossRef](#)]
21. Fragiaco, P.; Genovese, M. Technical-economic analysis of a hydrogen production facility for power-to-gas and hydrogen mobility under different renewable sources in Southern Italy. *Energy Convers. Manag.* **2020**, *223*, 113332. [[CrossRef](#)]
22. Lee, S.; Na, U.J.; Jo, H. Techno-economic assessment of green hydrogen production via two-step thermochemical water splitting using microwave. *Int. J. Hydrogen Energy* **2023**, *48*, 10706–10723. [[CrossRef](#)]
23. Babarit, A.; Gilloteaux, J.-C.; Clodic, G.; Duchet, M.; Simoneau, A.; Platzer, M.F. Techno-economic feasibility of fleets of far offshore hydrogen-producing wind energy converters. *Int. J. Hydrogen Energy* **2018**, *43*, 7266–7289. [[CrossRef](#)]
24. Ibagón, N.; Muñoz, P.; Díaz, V.; Teliz, E.; Correa, G. Techno-economic analysis for off-grid green hydrogen production in Uruguay. *J. Energy Storage* **2023**, *67*, 107604. [[CrossRef](#)]
25. Jang, D.; Kim, J.; Kim, D.; Han, W.-B.; Kang, S. Techno-economic analysis and Monte Carlo simulation of green hydrogen production technology through various water electrolysis technologies. *Energy Convers. Manag.* **2022**, *258*, 115499. [[CrossRef](#)]
26. Ulleberg, Ø. Modeling of advanced alkaline electrolyzers: A system simulation approach. *Int. J. Hydrogen Energy* **2003**, *28*, 21–33. [[CrossRef](#)]
27. AEMO. Assumptions and Scenarios Report. 2021. Available online: <https://aemo.com.au/-/media/files/major-publications/isp/2021/2021-inputs-assumptions-and-scenarios-report.pdf?la=en> (accessed on 25 April 2023).
28. AEMO. Costs and Technical Parameter Review Consultation Report. Available online: https://www.aemo.com.au/-/media/files/electricity/nem/planning_and_forecasting/isp/2021/aurecon{-}-cost-and-technical-parameters-review-2020.pdf?la=en (accessed on 27 May 2023).

29. Graham, P.; Hayward, J.; Foster, J.; Havas, L. *GenCost 2021–2022: Consultation Draft*; Commonwealth Scientific and Industrial Research Organisation (CSIRO): Canberra, Australia, 2021.
30. Bruce, S.; Temminghoff, M.; Hayward, J.; Schmidt, E.; Munnings, C.; Palfreyman, D.; Hartley, P. *National Hydrogen Roadmap*; CSIRO: Canberra, Australia, 2018.
31. Khan, M.H.A.; Daiyan, R.; Han, Z.; Hablutzel, M.; Haque, N.; Amal, R.; MacGill, I. Designing optimal integrated electricity supply configurations for renewable hydrogen generation in Australia. *IScience* **2021**, *24*, 102539. [CrossRef]
32. Balasubramanian, V.; Haque, N.; Bhargava, S.; Madapusi, S.; Parthasarathy, R. Techno-Economic Evaluation Methodology for Hydrogen Energy Systems. In *Bioenergy Resources and Technologies*; Elsevier: Amsterdam, The Netherlands, 2021; pp. 237–260.
33. IEA (International Energy Agency). *The Future of Hydrogen: Seizing Today's Opportunities*. 2019. Available online: https://iea.blob.core.windows.net/assets/9e3a3493-b9a6-4b7d-b499-7ca48e357561/The_Future_of_Hydrogen.pdf (accessed on 24 April 2023).
34. Brinsmead, T.S.; Hayward, J.; Graham, P. *Australian Electricity Market Analysis Report to 2020 and 2030*; CSIRO Technical Report No. EP141067; CSIRO: Canberra, Australia, 2014.
35. Khan, M.A.; Young, C.; Mackinnon, C.; Layzell, D. The Techno-Economics of Hydrogen Compression. *Tech. Briefs Can. Transit. Accel.* **2021**, *1*, 1e36.
36. CPI Inflation Calculation. 2019. Available online: <https://www.officialdata.org/us/inflation/2013?endYear=2019&amount=567> (accessed on 18 March 2023).
37. Inflation Calculator. Inflation Calculator for Canadian Dollar. 2023. Available online: <https://www.bankofcanada.ca/rates/related/inflation-calculator/#:~:text=The%20Inflation%20Calculator%20uses%20monthly,this%20cost%20is%20called%20inflation> (accessed on 22 March 2023).
38. ROAM Consulting. *Projections of Electricity Generation in Australia to 2050*. 2011. Available online: <https://treasury.gov.au/sites/default/files/2019-03/c2011-sglp-supplementary-ROAM.pdf> (accessed on 26 March 2023).
39. Build Australia. *Australia Becomes the Fourth Most Expensive Region for Construction Labour: Global Report*. 2022. Available online: https://www.buildaustralia.com.au/news_article/australia-becomes-the-fourth-most-expensive-region-for-construction-labour-global-report/ (accessed on 17 March 2023).
40. Haug, P.; Koj, M.; Turek, T. Influence of process conditions on gas purity in alkaline water electrolysis. *Int. J. Hydrogen Energy* **2017**, *42*, 9406–9418. [CrossRef]
41. De Atholia, T.; Flannigan, G.; Lai, S. *Renewable Energy Investment in Australia | Bulletin—March 2020*; Reserve Bank of Australia: Sydney, Australia, 2020.
42. Parks, G. *Hydrogen Station Compression, Storage, and Dispensing Technical Status and Costs*; National Renewable Energy Laboratory: Golden, CO, USA, 2014.
43. Barthélémy, H.; Weber, M.; Barbier, F. Hydrogen storage: Recent improvements and industrial perspectives. *Int. J. Hydrogen Energy* **2017**, *42*, 7254–7262. [CrossRef]
44. Tarhan, C.; Çil, M.A. A study on hydrogen, the clean energy of the future: Hydrogen storage methods. *J. Energy Storage* **2021**, *40*, 102676. [CrossRef]

Disclaimer/Publisher's Note: The statements, opinions and data contained in all publications are solely those of the individual author(s) and contributor(s) and not of MDPI and/or the editor(s). MDPI and/or the editor(s) disclaim responsibility for any injury to people or property resulting from any ideas, methods, instructions or products referred to in the content.